Revista Mexicana de Astronomía y Astrofísica, **46**, 179–184 (2010)

HH JETS ALIGNED PERPENDICULAR TO ELEPHANT TRUNKS

A. C. Raga,[1] V. Lora,[2] and N. Smith[3]

Received 2010 January 11; accepted 2010 February 15

RESUMEN

Consideramos un sistema the flujos eyectados por estrellas de baja masa sumergidas en las puntas de las "trompas de elefante". Suponemos que estos flujos tienen ejes que son intrínsecamente perpendiculares a los ejes de las trompas de elefante. Entonces, derivamos la función de distribución esperada para el ángulo entre las proyecciones sobre el plano del cielo de los ejes del flujo y de la trompa de elefante. Estas funciones de distribución son útiles para interpretar los alineamientos (o falta de alineamientos) observados entre los ejes de flujos HH y trompas de elefante en regiones fotoionizadas.

ABSTRACT

We consider a system of outflows ejected from low mass young stars embedded in the tips of elephant trunks. We assume that these outflows have axes which are intrinsically perpendicular to the axes of the host elephant trunks. We then derive the distribution function expected for the angle between the projections of the outflow and elephant trunk axes on the plane of the sky. These distribution functions are useful for interpreting the alignments (or lack thereof) observed between HH outflow and elephant trunk axes in photoionized regions.

Key Words: ISM: Herbig-Haro objects — ISM: jets and outflows — ISM: kinematics and dynamics — stars: formation

1. INTRODUCTION

"Elephant trunks" are elongated neutral/molecular structures located at the outer boundaries of H II regions (see, e. g., Carlqvist, Gahm, & Kristen 2003; Gahm et al. 2006). Low mass stars are being formed within these structures, and the HH outflows ejected by some of these stars emerge from the elephant trunks into the H II region. These regions are of clear interest in the context of the idea of "sequential star formation" (see, e. g., Elmegreen 1998) and have recently been modeled numerically (Mellema et al. 2006; Gritschneder et al. 2009; Mackey & Lim 2010).

Several cases of outflows ejected from low mass, young stars embedded in the tips of elephant trunks or other elongated structures have been reported in the literature. Examples of this are HH 555 (in the Pelican Nebula, see Bally & Reipurth 2003; Kajdič & Raga 2007) and HH 666 (in the Carina Nebula, see Smith, Bally, & Brooks 2004). These two outflows have orientations almost perpendicular to the axes of the elephant trunks (themselves aligned in the direction of the photoionizing sources).

These observations motivated the work of Lora, Raga, & Esquivel (2009), who used 3D gasdynamic+radiative transfer simulations to model the formation of an elephant trunk through the interaction of an impinging ionizing photon field and an environment with an inhomogeneous density structure. From their simulations, Lora et al. (2009) found that the vorticity of the more massive clumps formed by this interaction is preferentially aligned perpendicular to the direction towards the ionizing photon source. They suggested that the gravitational collapse of these clumps would result in accretion disks with orbital axes perpendicular to the axis of the elephant trunk (which is parallel to the direction towards the photoionizing source), producing jets along the disk axes.

In the present paper, we explore the observational signatures of jets with axes intrinsically perpendicular to the axes of the elephant trunks in

[1]Instituto de Ciencias Nucleares, Universidad Nacional Autónoma de México, Mexico.
[2]Instituto de Astronomía, Universidad Nacional Autónoma de México, Mexico.
[3]Department of Astronomy, University of California, Berkeley, USA.

which the outflow sources are embedded (see § 2). In particular, we derive the distribution functions predicted for the observed angle α between the projections of the outflow and elephant trunk axes on the plane of the sky. We consider the case of a localized system of elephant trunks (which share approximately the same orientation angle with respect to the line of sight, see § 3) and the case of a system of elephant trunks with arbitrary orientations (see § 4).

Our work is motivated by the recent paper of Smith, Bally, & Walborn (2010), who present a survey of outflows in the Carina Nebula. These authors derive the distribution of projected angles α between outflow axes and the elongated, neutral structures (in which the outflow sources are embedded) for a number of outflows, obtaining for the first time a quantitative evaluation of the statistical distribution of this angle. We use the theoretical distribution functions that we have derived in order to model the observed angular frequency distribution of Smith et al. (2010) (see § 5).

2. THE GEOMETRY OF THE PROBLEM

It is clear that if the elephant trunk lies on the plane of the sky, the observed, projected angle between the elephant trunk and the outflow axis is always $\alpha = \pi/2$. Also, if the elephant trunk lies close to the line of sight, the angle between the projected directions (on the plane of the sky) of the elephant trunk and the outflow axis will have any value $0 \le \alpha \le \pi/2$.

The geometry of the problem for an arbitrary orientation θ between the elephant trunk and the line of sight is shown in Figure 1. We consider a coordinate system with the z-axis along the line of sight, and the x-axis parallel to the projection of the elephant trunk on the plane of the sky.

The bipolar outflow is ejected perpendicular to the elephant trunk. The direction of the ejection is determined by the angle θ (between the elephant trunk and the line of sight, see Figure 1) and the angle ϕ, measured on the plane defined by the rotation of the ejection direction around the elephant trunk axis. As is clear from Figure 1, for $\phi = 0$ the outflow axis lies on the xz-plane, and for $\phi = \pi/2$ the outflow coincides with the y-axis. We define the angle α ($0 \le \alpha \le \pi/2$) between the x-axis and the projection on the plane of the sky of the outflow axis (see Figure 1).

From the geometry of the problem, one finds the relations :

$$\sin\alpha = \frac{\sin\phi}{\sqrt{1-\sin^2\theta\cos^2\phi}}\,, \tag{1}$$

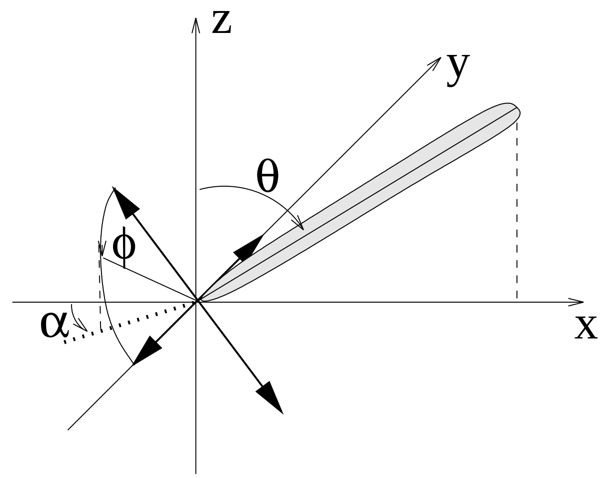

Fig. 1. Schematic diagram showing a bipolar outflow system (two possible directions shown by the thick, double arrows) ejected from a source located at the tip of an elephant trunk (grey, elongated structure at an angle θ with respect to the z-axis). The z-axis lies along the line of sight, the xy-plane is parallel to the plane of the sky, and the x-axis is located along the plane of the sky projection of the elephant trunk. The outflow axis is perpendicular to the axis of the elephant trunk, and can be rotated at an angle ϕ around the elephant trunk axis (with the outflow axis on the xz-plane for $\phi = 0$). The angle α is measured between the x-axis and the projection of the outflow axis on the xy-plane.

$$\sin\phi = \frac{\sin\alpha}{\sqrt{1-\tan^2\theta\cos^2\alpha}}\,, \tag{2}$$

between the angles α, θ and ϕ.

3. DISTRIBUTION OF THE PROJECTED ANGLES FOR A LOCALIZED SYSTEM OF ELEPHANT TRUNKS

We now assume that we have a localized system of elephant trunks, so that they all have approximately the same angle θ with respect to the line of sight. Then, if the "rotation angle" ϕ (see Figure 1) is uniformly distributed (between 0 and π), the angle α (between the projected outflow and elephant trunk axes) will have a distribution

$$D_\theta(\alpha) = \frac{2}{\pi}\frac{d\phi}{d\alpha} = \frac{2}{\pi}\frac{\cos\theta}{\cos^2\theta+\sin^2\theta\cos^2\alpha}\,, \tag{3}$$

where $d\phi/d\alpha$ is calculated for a constant θ from equations (1, 2). This distribution function is normalized so that

$$\int_0^{\pi/2} D_\theta(\alpha)d\alpha = 1\,. \tag{4}$$

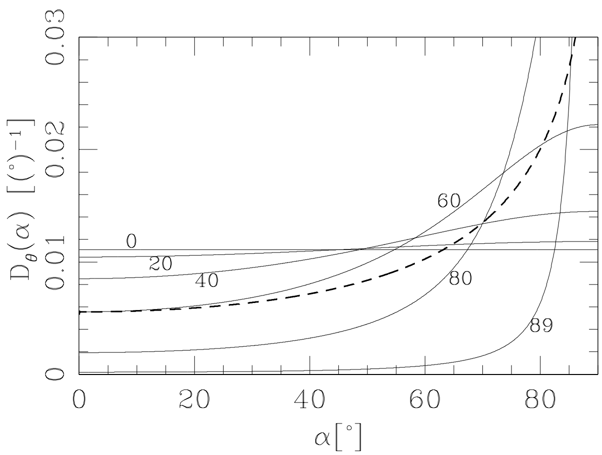

Fig. 2. The solid lines represent the distribution function function $D_\theta(\alpha)$ (where α is the angle between the plane of the sky projections of the outflow and elephant trunk axes) for values of the orientation angle $\theta = 0$, 20, 40, 60, 80 and 89° between the elephant trunks and the line of sight (see equation 3). The dashed line gives $D(\alpha)$ (see equation 9) derived for a system of elephant trunks with randomly distributed directions. The distribution functions as shown (in units of $[^\circ]^{-1}$) are obtained by multiplying equations (3) and (9) by a factor of $\pi/180^\circ$.

Figure 2 shows the $D_\theta(\alpha)$ distribution for different values of the orientation θ between the elephant trunks and the line of sight. For $\theta = 0$, a uniform distribution is obtained, and for $\theta \to 90^\circ$, the distribution has a strong peak at $\alpha = 90^\circ$. We see from Figure 2 that for $\theta < 45^\circ$ the $D_\theta(\alpha)$ distributions are quite flat, indicating that one will not see a significant preferential alignment between the plane of the sky projections of the outflow and elephant trunk axes.

However, for $\theta \geq 60^\circ$ (see Figure 2), the fact that the outflow and elephant trunk axes are intrinsically perpendicular to each other is indeed reflected on the distribution of the projected angle α between the two axes. Therefore, in order to be able to test observationally whether or not the outflow and elephant trunk axes are intrinsically perpendicular to each other, it is essential to choose elephant trunks which lie close to the plane of the sky.

Let us now calculate the average projected angle

$$< \alpha > (\theta) = \int_0^{\pi/2} \alpha D_\theta(\alpha) d\alpha \,, \tag{5}$$

and the dispersion

$$\sigma(\theta) = \sqrt{\int_0^{\pi/2} \left[\alpha - < \alpha > (\theta)\right]^2 D_\theta(\alpha) d\alpha} \,. \tag{6}$$

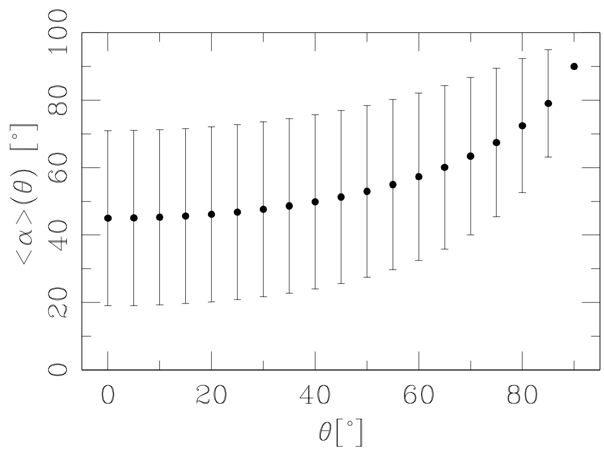

Fig. 3. The mean value (dots) $< \alpha > (\theta)$ and standard deviation (error bars) $\sigma(\theta)$ (see equations 5 and 6, respectively) derived for the $D_\theta(\alpha)$ distributions (see equation 3) as a function of the angle θ between the elephant trunks and the line of sight. For $\theta = 90^\circ$, we have $< \alpha >= 90^\circ$ and $\sigma = 0$.

The results obtained from numerical integrations of equations (5, 6) are shown in Figure 3. In this figure, we see that $< \alpha > (\theta)$ monotonically grows from 45° (for $\theta = 0$) to 90° (for $\theta = 90^\circ$). The dispersion $\sigma(\theta)$ monotonically decreases from 26° (for $\theta = 0$) to 0 (for $\theta = 90^\circ$).

As can be seen from Figure 3, both $< \alpha > (\theta)$ and $\sigma(\theta)$ are almost constant for low values of θ, and have a stronger dependence on θ when $\theta \to 90^\circ$. This is a direct result of the fact that the $D_\theta(\alpha)$ distribution function (see equation 3) shows substantial departures from a uniform distribution only for $\theta \geq 60^\circ$ (see Figure 2).

4. RANDOMLY DISTRIBUTED ELEPHANT TRUNKS

Let us now assume that we have a system of elephant trunks with randomly distributed orientations with respect to the plane of the sky. This situation could be obtained if we observe elephant trunks associated with a shell-like structure completely surrounding a photoionizing source.

If the elephant trunks have uniformly distributed directions, the distribution $f(\theta)$ of the angle θ with respect to the line of sight follows the relation $f(\theta)d\theta \propto d\Omega$, from which we obtain

$$f(\theta) = \sin\theta \,, \tag{7}$$

using the normalization

$$\int_0^{\pi/2} f(\theta) d\theta = 1 \,. \tag{8}$$

The distribution $D(\alpha)$ of the angles between the plane of the sky projections of the outflows and the elephant trunks (see Figure 1) can then be calculated as

$$D(\alpha) = \int_0^{\pi/2} D_\theta(\alpha) f(\theta) d\theta = -\frac{2}{\pi \sin^2 \alpha} \ln(\cos \alpha) \,, \tag{9}$$

where for the second equality we have used equations (3) and (7).

This distribution function (see equation 9) is shown in Figure 3. It is flat for $\alpha \leq 50^\circ$, and has a logarithmically divergent peak for $\alpha \to 90^\circ$. Using equations (5, 6), we calculate a mean value $<\alpha>= 60^\circ$ and a dispersion $\sigma = 26^\circ$ for $D(\alpha)$ (see equation 9).

5. A COMPARISON WITH OBSERVATIONS

Smith et al. (2010) carried out an Hα survey of outflows in the Carina Nebula. In their images, they detect 22 outflows from sources embedded in elongated neutral structures, for which they determine the angles α between the elongated structures and the outflow axes. With these objects, they compute a frequency histogram of number of outflows with α values within 5° wide bins (Figure 34 of Smith et al. 2010). The resulting frequency diagram is quite noisy, with many bins having populations of 0 or 1 outflows only.

In order to compare the observations with the theoretical prediction (see § 4), we use the data from the angular distribution frequency histogram of Smith et al. (2010) to compute the cumulative angular distribution $f_o(\alpha) = P(\alpha' < \alpha)$ (i. e., the probability that the observed angle α' is smaller than a given projected angle α between the outflow and elephant trunk axes). The resulting empirical cumulative distribution function is shown in Figure 4.

We compare the empirical cumulative distribution $f_o(\alpha)$ with the one derived from the $D(\alpha)$ distribution (see equation 9):

$$f_c(\alpha) = \int_0^{\alpha} D(\alpha')\, d\alpha' = \frac{2}{\pi} \left[\alpha - \frac{\ln(\cos \alpha)}{\tan \alpha} \right] \,. \tag{10}$$

This distribution is shown in Figure 4 (solid curve). In this figure we also show the

$$f_u(\alpha) = \frac{2\alpha}{\pi} \,, \tag{11}$$

cumulative distribution that results from assuming that α is uniformly distributed in the $0 \to \pi/2$ range.

We find that the maximum discrepancy between $f_o(\alpha)$ (the observed cumulative distribution) and

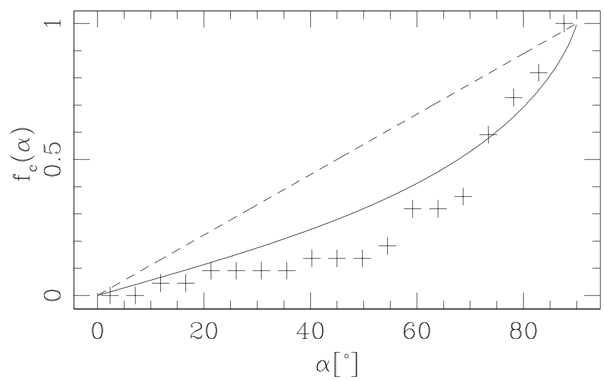

Fig. 4. Cumulative distribution functions (giving the probability of having a projected angle $< \alpha$ between the outflow and elephant trunk axes). The crosses show the cumulative distribution calculated from 22 outflows emerging from elongated, neutral host structures in the Carina Nebula outflow survey of Smith et al. (2010). The solid line corresponds to the $f_c(\alpha)$ cumulative distribution function derived for a system of elephant trunks at arbitrary orientations with respect to the plane of the sky (see § 4 and equation 10). The dashed line corresponds to the $f_u(\alpha)$ cumulative distribution function corresonding to a uniform frequency distribution (see equation 11).

$f_c(\alpha)$ (see equation 10) has a value $D_c = 0.22$. The maximum discrepancy between the observed cumulative distribution and the one predicted for a uniform angular distribution is $D_u = 0.476$. Using the Kolmogorov-Smirnov statistic (see, e. g., Press et al. 2007), these discrepancies can be shown to correspond to probabilities $P_c = 0.27$ and $P_u = 2.0 \times 10^{-4}$ that the data have equal or larger offsets with respect to the chosen distributions (f_c and f_u, respectively, see equations 10 and 11).

These results imply that the data indeed appear to be inconsistent with a uniformly distributed angle α between the outflow and elephant trunk axes. The agreement between the $f_c(\alpha)$ distribution predicted from our model (for a set of elephant trunks with random orientations with respect to the plane of the sky, see § 4 and equation 10) and the data is appreciably better than the one obtained for a uniform distribution (see Figure 4 and the discussion above).

6. CONCLUSIONS

In this paper we evaluate the implications for observations of the hypothesis that jets from young stars in the tip of elephant trunks are ejected perpendicular to the body of the trunks. To this effect, we compute the expected distribution function of the angle α between the projections on the plane of the sky of the outflow and elephant trunk axes.

We find that if the elephant trunk lies close to the line of sight ($\theta \sim 0$, see Figure 1), one obtains an approximately uniform distribution of α within $0 \to 90°$ (see Figure 2). Therefore, for such an orientation of the elephant trunk, the information that the outflow is perpendicular to the trunk is lost.

On the other hand, for an elephant trunk close to the plane of the sky ($\theta \sim 90°$, see Figure 1), the predicted distribution function has a strong peak at $\alpha = 90°$. Therefore, for elephant trunks on the plane of the sky, one would expect to see outflows with projected orientations approximately perpendicular to the elephant trunk axes.

We have also computed the distribution function for a system of elephant trunks at arbitrary orientations with respect to the line of sight. The resulting distribution (see Figure 2) has a logarithmically divergent peak at $\alpha = 90°$, and results in an average orientation angle $<\alpha>= 60°$, with a standard deviation $\sigma = 26°$ (for the individual outflows).

In order to illustrate a possible comparison with observations, we consider the sample of 22 outflows in the Carina Nebula for which Smith et al. (2010) have computed the α angles between the projected axes of the outflows and the elongated, neutral host structures from which they emanate (see § 5). From these data we compute a cumulative angular distribution function, which we compare with the predictions from our model (for the case of a set of randomly oriented elephant trunks described in § 4) and with the predictions for a uniform angular distribution. We find that the data are in statistically significant disagreement with a uniform angular distribution, and that they are in better agreement with the predictions from our $D(\alpha)$ distribution (see equations 9 and 10).

More satisfying results might be obtained if one restricted the observational sample to a group of elephant trunks which lie close to the plane of the sky. For such a case ($\theta \sim 90°$, see Figure 1), if the outflow axes are intrinsically perpendicular to the host elephant trunks one should also clearly see projected angles $\alpha \sim 90°$ (see the $\theta = 80°$ and $90°$ distributions in Figure 2). It is possible that the elephant trunks from which emerge the impressively aligned HH 901 and HH 902 systems (see Figure 5 of Smith et al. 2010) are an example of such a system.

In order to progress further, it will be necessary to obtain observations constraining the orientation with respect to the line of sight of elephant trunks. It might be possible to obtain such constraints purely from an analysis of the brightness distribution of the emission from the outer, photoionized skins of the elephant trunks. However, kinematical information might prove to be essential for constraining the orientation of the elephant trunks.

Such observations could, of course, be combined with radial velocity and proper motion determinations of the outflow in order to directly obtain the true (de-projected) angle between the outflow and elephant trunk axes. This type of determination would directly tell us whether a mechanism leading to a preferential ejection perpendicular to the elephant trunk (such as the one studied by Lora et al. 2009) is indeed present.

We end our discussion by noting that all of the distributions derived in the present paper are for outflows which are intrinsically ejected at right angles to the axis of the elongated, neutral structure (in which the outflow source is embedded). Mechanisms producing such an (anti-) alignment, however, are likely to produce a range of orientations, all of them forming angles of close to 90° between the two axes (this is the case, e. g., of the simulations of Lora et al. 2009, which predict angles larger than $\sim 80°$). This intrinsic dispersion in the angle between the outflow and elephant trunk axes will result in distributions with broader peaks than the $D_\theta(\alpha)$ and $D(\alpha)$ distributions discussed in §§ 3 and 4.

The work of AR and VL was supported by Conacyt grants 61547, 101356 and 101975 and DGAPA-Universidad Nacional Autónoma de México grant IN119709. NS was supported by NASA through grants GO-10241 and GO-10475 from the Space Telescope Science Institute, which is operated by the Association of Universities for Research in Astronomy, Inc., under NASA contract NAS5-26555. We thank an anonymous referee for comments which led to a complete rework of § 5.

REFERENCES

Bally, J., & Reipurth, B. 2003, AJ, 126, 893

Carlqvist, P., Gahm, G. F., & Kristen, H. 2003, A&A, 403, 399

Elmegreen, B. G. 1998, in ASP Conf. Ser. 148, Origins, ed. C. E. Woodward, J. M. Shull, & H. A. Thronson, Jr. (San Francisco: ASP), 150

Gahm, G. F., Carlqvist, P., Johansson, L. B., & Nicolić, S. 2006, A&A, 454, 201

Gritschneder, M., Naab, T., Walch, S., Burkert, A., & Heitsch, F. 2009, ApJ, 694, L26

Kajdič, P., & Raga, A. C. 2007, ApJ, 670, 1173

Lora, V., Raga, A. C., & Esquivel, A. 2009, A&A, 503, 477

Mackey, J., & Lim, A. J. 2010, MNRAS, in press

Mellema, G., Arthur, S. J., Henney, W. J., Iliev, I. T., & Shapiro, P. R. 2006, ApJ, 647, 397
Press, W. H., Teukolsky, S. A., Vetterling, W. T., & Flannery, B. P. 2007, Numerical Recipes (Cambridge: Cambridge Univ. Press)
Smith, N., Bally, J., & Brooks, K. 2004, AJ, 127, 2793
Smith, N., Bally, J., & Walborn, N. R. 2010, MNRAS, (submitted)

Alejandro C. Raga: Instituto de Ciencias Nucleares, Universidad Nacional Autónoma de México, Apdo. Postal 70-543, 04510 D. F., Mexico (raga@nucleares.unam.mx).
Verónica Lora: Instituto de Astronomía, Universidad Nacional Autónoma de México, Apdo. Postal 70-548, 04510 D. F., Mexico (vlora@astroscu.unam.mx).
Nathan Smith: Department of Astronomy, University of California, Berkeley, CA 94720, USA (nathans@astro.berkeley.edu).